HYDRAULIC JUMP ON CORRUGATED BEDS

A DISSERTATION

Submitted in partial fulfillment of the requirements for the award of the degree
of
MASTER OF TECHNOLOGY
in
CIVIL ENGINEERING
(With Specialization in Hydraulic Engineering)

By

PRADEEP KUMAR YADAV

DEPARTMENT OF CIVIL ENGINEERING
INDIAN INSTITUTE OF TECHNOLOGY ROORKEE
ROORKEE-247 667 (INDIA)

JUNE, 2006

CANDIDATE'S DECLARATION

I hereby certify that the work which is being presented in the dissertation entitled **"HYDRAULIC JUMP ON CORRUGATED BEDS"** in partial fulfillment of the requirements for the award of the degree of **Master of Technology** in **Civil Engineering** with specialization in Hydraulic Engineering, submitted in the Department of Civil Engineering, **Indian Institute Of Technology Roorkee, Roorkee** is an authentic record of my own work carried out from September 2005 to June 2006 under the supervision of **Dr. G. L. Asawa,** Professor & Head, Department of Civil Engineering, I.I.T Roorkee and **Dr. Z. Ahmad,** Asst. Professor, Department of Civil Engineering, I.I.T Roorkee.

The matter embodied in this dissertation has not been submitted by me for the award of any other degree.

Date: 30 June, 2006

Place: Roorkee

(PRADEEP KUMAR YADAV)

CERTIFICATE

This is to certify that above statement made by the candidate is correct to the best of my knowledge.

Dr. Z. Ahmad
Asst. Professor,
Department of Civil Engineering,
IIT Roorkee
Roorkee-247667

Dr. G. L. Asawa
Professor & Head,
Department of Civil Engineering,
IIT Roorkee
Roorkee-247667

ACKNOWLEDGEMENT

I wish to express my deep gratitude and sincere thanks to **Dr. G. L. Asawa**, Professor and Head, Department of Civil Engineering, IIT Roorkee and **Dr. Z. Ahmad**, Assistant Professor, Department of Civil Engineering, IIT Roorkee for their generous help, guidance and co-operation at every step throughout this work. They provided much of their valuable time, skills and knowledge to me with great pleasure and always encouraged me to achieve my objective. I am highly indebted to them and fortunate for having worked under their supervision. The huge quantum of knowledge I had gained during their inspiring guidance would be immensely beneficial for my future endeavours.

I acknowledge the blessing of my parents and cooperation of my friends. I am also thankful to the staff of Hydraulic Engineering Section who stood by me during the dissertation work.

Dated: 30 June 2006.

Place: Roorkee.

Pradeep Kumar Yadav

ABSTRACT

The hydraulic jump used for energy dissipation is usually confined entirely to a channel reach known as the stilling basin. The bottom of the basin is paved to resist scouring. Designing a stilling basin for a given hydraulic structure involves considerations of parameters peculiar to the location of the structure in addition to the mechanics of flow. This feature makes the engineering design to rely rather heavily on the experience of the designer. In practice, the stilling basin is seldom designed to confine the entire length of a free hydraulic jump on the paved apron, because such a basin would be too expensive. Consequently, accessories to control the jump are usually installed in the basin. The main purpose of such control is to shorten the range within which the jump will take place and thus to reduce the size and cost of the stilling basin. The control has additional advantages, for it improves the dissipation function of the basin, stabilizes the jump action, and in some cases increases the factor of safety. Stilling basins should be so designed that not only a good jump with high energy-dissipation characteristics is formed within the basin but it also is stable. The appurtenances in traditional stilling basins include baffle blocks and sills to aid in the efficient performance over a wide range of operating conditions. In the present work, the corrugated beds as an alternative to the traditional control accessories have been studied.

Ead and Rajaratnam (2002) through experiments with hydraulic jumps on corrugated beds for relative roughness t/y_1 values of 0.50, 0.43 and 0.25 and Froude numbers ranging from 4 to 10 showed that the tailwater depth required to form a jump was found to be appreciably smaller than that for the corresponding jumps on a smooth bed. Also the length of the jumps was about half of those on smooth bed. The integrated bed shear stress on the corrugated bed was about ten times that on smooth bed.

In the present study, further experiments are performed to evaluate the effect of relative roughness t/y_1 over a larger range and the effect of the wavelength(s) of the corrugations. The values of t/y_1 chosen are 0.55, 0.6, 0.65, 0.7, 0.75; s/y_1 values from 1.36 to 3.75 and Froude number ranging from 1.7 to 7. The results supported the previous findings pointing towards the usefulness of the corrugations in stabilizing the jumps.

LIST OF FIGURES

LIST OF PHOTOGRAPHS

LIST OF TABLES

LIST OF SYMBOLS

Symbol		Description
B	=	downstream channel width
b_o	=	slot width
b	=	width of the channel
Ef_1 and Ef_2	=	pre-jump and post-jump specific energies
F_τ	=	integrated bed shear stress, per unit width, over jump length
F_1	=	supercritical Froude number
F_2	=	subcritical Froude number
g	=	acceleration due to gravity
ΔH	=	mechanical head loss
H_1	=	approach energy head
h	=	weir height
L_{j^*}	=	length of jump on smooth bed
L_j	=	length of jump on corrugated bed
L_{rj}	=	length of surface roller
M_1	=	momentum flux, per unit width, at section where jump starts
M_2	=	momentum flux, per unit width, at section where jump ends
P_1	=	hydrostatic force, per unit width, at section where jump starts
P_2	=	hydrostatic force, per unit width, at section where jump ends
Q	=	discharge
q	=	discharge intensity equal to Q/b
R_1	=	Reynolds number
S	=	relative step size
s'	=	rise or drop
s	=	wavelength of corrugations

t = corrugation height from crest to trough

U_1 = depth-averaged velocity at section where jump starts

U_2 = depth-averaged velocity at section where jump ends

u_m = maximum value of u at any station x

X = distance from the toe of the jump to the weir

x = longitudinal distance measured from section where jump starts

Y = sequent depth ratio

y = distance from crest of corrugations

y_1 = supercritical initial depth of free jump

y_2 = subcritical depth of jump on corrugated bed

y_{2*} = subcritical sequent depth of classical jump

α_j = constant

β = width ratio

δ = boundary layer thickness

ε = shear force coefficient equal to F_τ/P_1

ε_1 = shear force coefficient equal to F_τ/M_1

η = efficiency of jump

μ = dynamic viscosity of fluid

ρ = mass density of fluid

τ = bed shear stress

CONTENTS

Chapter1

INTRODUCTION

1.1 General

Hydraulic jump is one subject which has been extensively studied in the field of hydraulic engineering. It was first described by Leonardo da Vinci in the sixteenth century. Bidone (1818), an Italian engineer carried out the first experimental investigation of this phenomenon. Since then this intriguing and interesting phenomenon has been studied by a number of researchers. Significant contributions are due to Belanger in 1838, Bazin and Darcy in 1865, and Boussinesq in 1877. The concept of sequent depths was generally accepted around 1930 when Safranez published his results. Various elements of flow were analysed, including the height and length of the jump, the shape of the free surface, the velocity profiles, the turbulence and pressure characteristics, and the air entrainment. Up to the mid-Seventies, all studies were experimental because of the complex two-phase flow and high degree of turbulence. The first computational models were developed by Narayan (1975), McCorquodale and Khalifa (1983) and Madsen and Svendsen (1983). Although there exist hundreds of papers on jumps, knowledge is incomplete and research in this domain of hydraulics continues (Hager, 1995).

1.1.1 Definition

Hydraulic jump also known as a standing wave results where there is a conflict between upstream and downstream control. The upstream control causes supercritical flow while the downstream control dictates subcritical flow. The conflict can be resolved only if there is some means for the flow to pass from one regime to another. Experimental evidence suggest that flow changes from supercritical to subcritical very abruptly through a phenomenon known as a hydraulic jump (Photograph 1.1). Thus, a hydraulic jump can be defined as a rapidly varied transition from supercritical to subcritical flow in an open channel. It is the basic phenomenon used to dissipate excess hydrodynamic energy, mainly into heat (Hager, 1995).

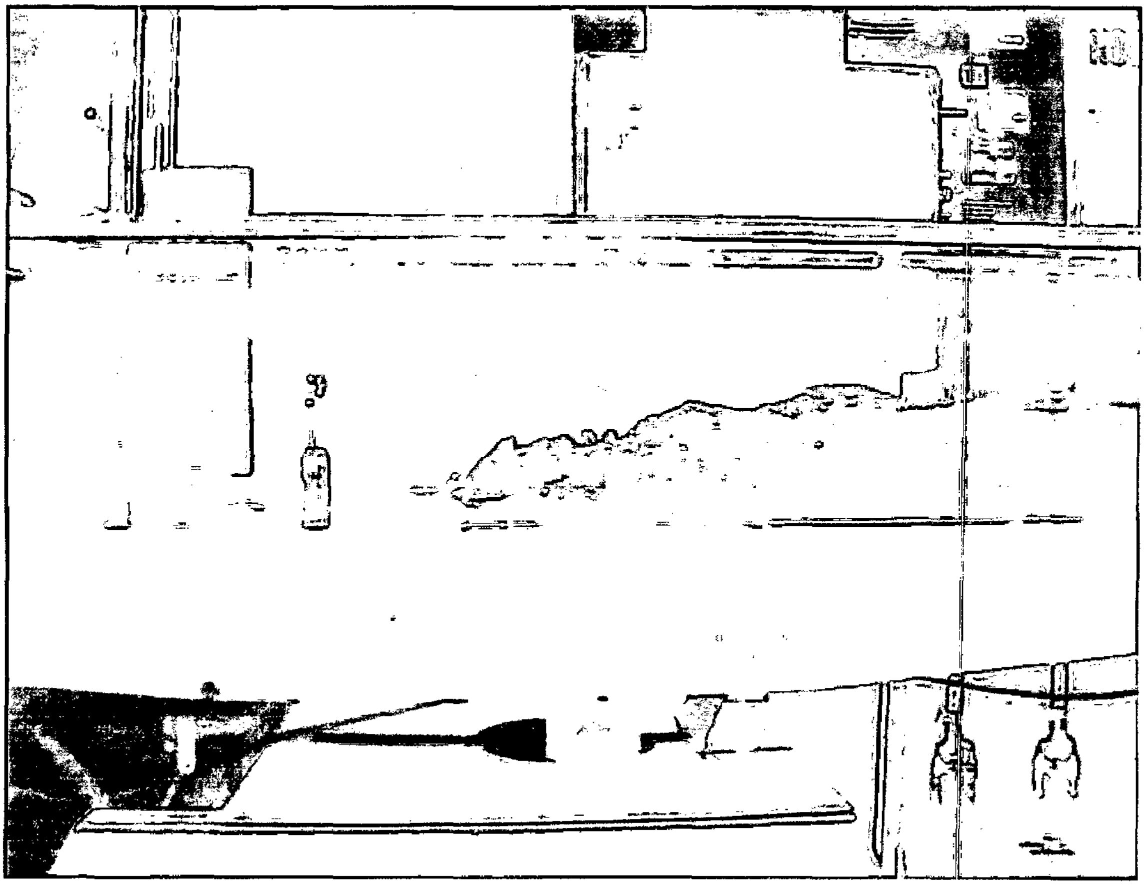

Photograph 1.1 Hydraulic Jump (www.google.com)

The features of a hydraulic jump are:

- highly turbulent flow,
- pulsation in the body of jump,
- generation of tailwater waves,
- air entrainment,
- energy dissipation due to turbulence production,
- erosive potential, and
- generation of spray and sound.

The hydraulic jump may appear in two different ways:

- either with a *varying* location in a channel, depending on the boundary conditions,
- or as a means to dissipate excess energy in a stilling basin with a *fixed* location.

The hydraulic jump can take place either on free surface of homogeneous flow or a density interface in stratified flow. In either case, the hydraulic jump is accompanied by significant turbulence and energy dissipation. The high velocity flows as well as the jump itself have excessive scouring potential and thus stilling basin design requires provision of a concrete apron underneath the jump and the supercritical stream (Hager, 1995).

1.1.2 Types of Jump

In a hydraulic jump, if the tailwater depth is less than the conjugate depth corresponding to the pre-jump depth, the jump is repelled down while if the tailwater depth is greater than the conjugate depth corresponding to the pre-jump depth, the jump moves upstream and in some situations the jump is no longer free but gets drowned (Ranga Raju, 1993).

The United States Bureau of Reclamation (USBR) has made extensive studies of the types of jump obtained at different Froude numbers. It has classified hydraulic jumps formed in horizontal rectangular channels into five categories based on the Froude number F_1 of the upstream supercritical flow, as follows (Subramanya, 1989):

1. <u>Undular Jump</u>: $1 < F_1 \leq 1.7$

The change from the supercritical state to the subcritical state is not abrupt and only a slightly ruffled water surface is obtained. The sequent-depth ratio is very small and efficiency of the jump $\eta = \Delta H/H_1$, defined as the mechanical head loss ΔH normalized by the approach energy head $H_1 = y_1 + Q^2/(2gb^2y_1^2)$, is nearly equal to zero.

2. Weak Jump: $1.7 < F_1 \leq 2.5$

The surface roller develops at $F_1 \approx 1.7$ and gradually increases in intensity towards the end of this range. The energy dissipation is small, η is about 5 percent at $F_1 = 1.7$ and 18 percent at $F_1 = 2.5$. The downstream water surface remains smooth.

3. Oscillating Jump: $2.5 < F_1 \leq 4.5$

An instable high velocity flow oscillating in a random manner between the bed and the surface forms the characteristic feature of these types of jumps. The oscillations produce large surface waves which travel downstream. Energy dissipation is moderate; $\eta = 45$ percent at $F_1 = 4.5$.

4. Steady Jump: $4.5 < F_1 \leq 9$

The jump is fully established with energy loss ranging from 45 to 70 percent. The jump is least sensitive of the toe position to small fluctuations in the tailwater elevation.

5. Strong Jump: $F_1 > 9$

The water surface is rough and choppy. The water surface downstream is also wavy. The sequent-depth ratio is large and the energy dissipation may reach 85 percent.

The various types of the hydraulic jump are shown in Fig.1.1.

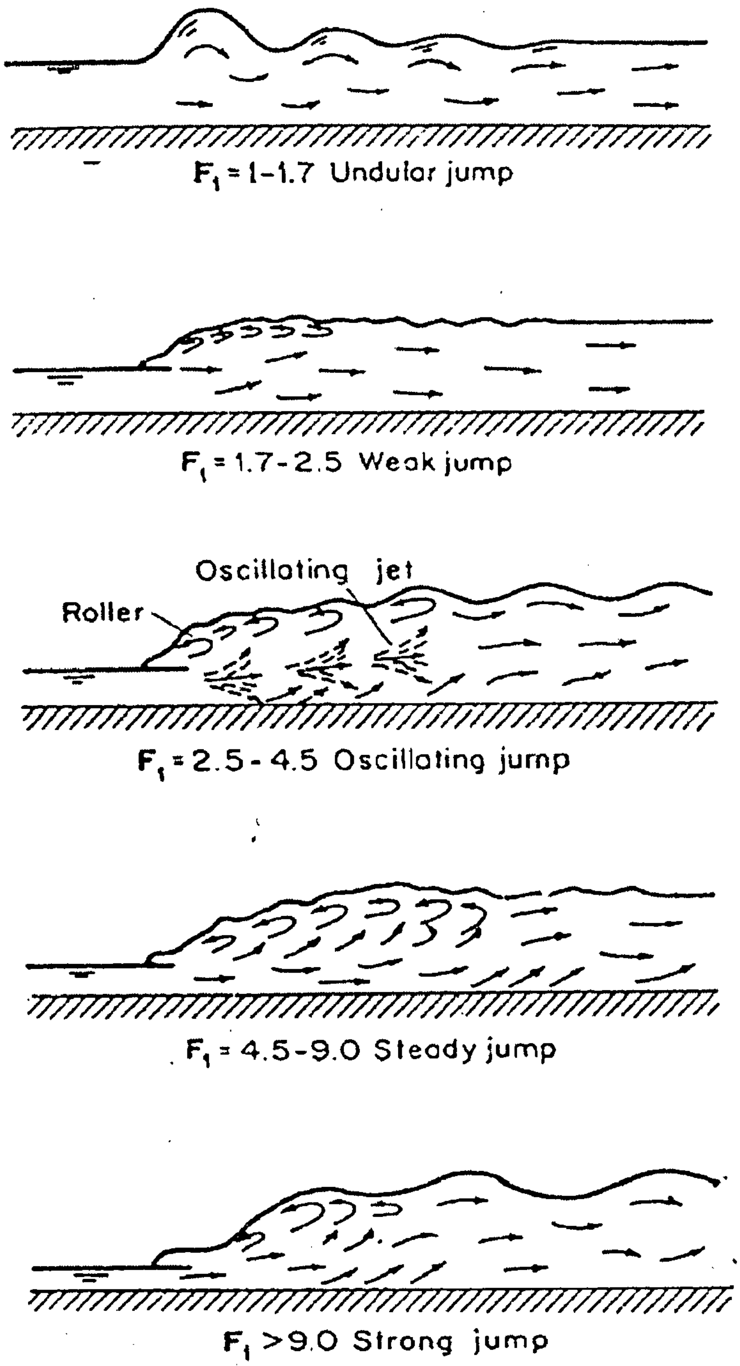

Fig.1.1. Various types of hydraulic jump (Chow, 1973)

1.1.3 Utility of Jump

The reason for such continued interest in this topic is its immense practical utility in hydraulics and allied fields. It is mainly used to dissipate excess energy of water flowing over dams, weirs, and other hydraulic structures and thus prevent objectionable scouring downstream of the structures. Some of the other uses of hydraulic jump are: (a) to recover head or raise the water level on the downstream side of a measuring flume and thus maintain high water level in the channel for irrigation; (b) to increase weight on an apron and thus reduce uplift pressure by raising the water depth on the apron; (c) to increase the discharge of a sluice by holding back tailwater; (4) to indicate special flow conditions, such as the existence of supercritical flow or the presence of a control section; (e) to mix chemicals used for water purification; (f) to aerate city water supplies and polluted streams; (g) to remove air pockets from water-supply lines and thus prevent air locking; and even (h) to desalinate sea water (Subramanya 1989).

1.2 Brief review of literature

There have been many investigations on the effect of the roughness elements on physical parameters of hydraulic jump. The investigations carried out by Rajaratnam (1968) indicated that, if the hydraulic jump is formed on a channel having rough bed, the tailwater depth y_2 required to form a jump could be appreciably smaller than the corresponding sequent depth y_{2*}. For a relative roughness of the bed in terms of the supercritical depth y_1 equal to about 0.4, y_2 could be as small as $0.8y_{2*}$, which is significant when it is realized that the tailwater depths required for Peterka's Basins II and III are 0.83 and 0.97 times y_{2*} [illegible], respectively. Studies by Hughes and Flack (1984) and Hager (1992) have supported this reduction in the required tailwater depth produced by the roughness of the bed. Rajaratnam (1968) further noticed that the length of the jumps on rough beds were significantly shorter than the classical jump.

In practice, baffle blocks and sills are commonly employed to stabilize the location of a jump and shorten the length of a stilling basin. The main problem with jumps on rough beds is that the roughness elements located in the upstream part of the jumps might be subjected to cavitation and possible scour, resulting in the movement of the jump to the downstream unprotected streambed, thus causing erosion and endangering the structure itself. The study by Ead et. al. (2000) on turbulent open channel flow in circular corrugated culverts indicated that the intense mixing induced by the corrugations produced significant Reynolds shear stresses in the plane of the crests of the corrugations and significant reduction in the velocity field above the corrugations. It looked that, if jumps were made to occur on corrugated beds, significant reductions might occur in the required tailwater depth and length of the jumps. Further, if the crests of the corrugations were at the level of the upstream bed carrying the supercritical stream, the corrugations would not be protruding into the flow and hence may not be subjected to the same intensity of cavitation as in the case of protruding roughness.

Recently an exploratory laboratory investigation was performed with hydraulic jumps on corrugated beds by Ead and Rajaratnam (2002) for relative roughness t/y_1 values of 0.50, 0.43 and 0.25 with Froude numbers ranging from 4 to 10. The tailwater depth required to form a jump was found to be noticeably smaller than that for the corresponding jumps on smooth beds. Also the length of the jumps was about half of those on smooth beds. The integrated bed shear stress on the corrugated bed was about ten times that on smooth beds. The results of the study showed that the idea of using corrugated beds for energy dissipation for hydraulic structures is a good one and needs much attention.

In the light of the observations of the above work and to gain a clear ground the idea of corrugated beds were explored further. The research was extended to get an insight into the effect of larger range of the relative roughness values and also to study the effect of the wavelength of the corrugations. The present study is devoted to help develop the theme of using the corrugated channel beds covering the basin as an effective parallel alternative to the accessory devices such as baffle blocks and sills.

1.3 Objectives of the present study

Previous study on corrugated bed reveals that corrugations of beds do affect the different parameters of hydraulic jump. However, those parameters of hydraulic jump were found invariable to the dimension of corrugation in the range of the data studied. The work of the previous investigators has been extended to examine the effect of corrugations on the different parameters of the jump for the wide range of the corrugation dimension.

Thus the following objectives were set for the present study-

a) To perform the experiment of hydraulic jump on both smooth and as well as the corrugated bed for different corrugation dimension.

b) To analyze the data collected in the present study and data of the previous investigators so as to examine the effect of the corrugation dimensions on the different parameters of hydraulic jump.

1.4 Limitations of the study

The following limitations were encountered during the course of the present study-

a) The corrugations of the fabricated sheets were not exactly sinusoidal.

b) The experiments could not be performed for higher values of Froude number due to the limitations on the discharge obtained from the pump.

REVIEW OF LITERATURE

2.1 General

A jump formed in a horizontal, wide rectangular channel with a smooth bed is often referred to as the classical hydraulic jump and has been studied extensively (Peterka 1958; Rajaratnam 1967; McCorquodale 1968; Hager 1992). The classical hydraulic jump is a basic physical phenomenon that is commonly used in stilling basin. In the present chapter the main characteristics of a hydraulic jump and different methods to control the jump are studied.

2.2 Characteristics of Classical Jump

Fig. 2.1 shows the definition sketch of a hydraulic jump. At the toe of the jump, the flow depth is y_1, and the average velocity is $U_1 = Q/(by_1)$ with Q = discharge and b = channel width. At the end of the jump the depth is y_{2*} and the velocity U_2.

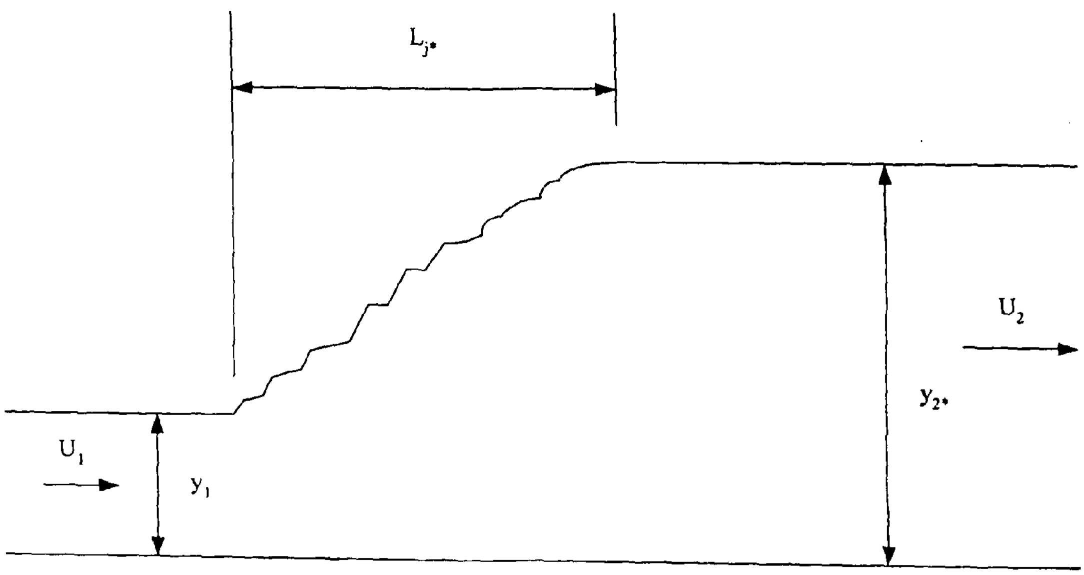

Fig.2.1 Definition sketch of hydraulic jump

The hydraulic jump is a quasi-steady phenomenon, although highly turbulent. The inflow jet is at the bottom in the region near the toe, and expands upward in the central part of the jump. Close to the free surface, the roller flow zone marked by a highly turbulent separation region with a return flow is located. At the end of the roller, the forward flow extends over the entire flow depth, and a surface stagnation point forms. Beyond the end of the jump, the flow is practically not disturbed by the formation of jump (Hager, 1995).

The ratio of sequent depths is a fundamental characteristic of the classical jump. Under the assumptions that: (a) the velocity distribution is uniform and the pressure distribution is hydrostatic at the two ends of the jump, (b) the bed is horizontal and the channel has a rectangular prismatic section, (c) the boundary shear stress is negligible, (d) effects of air entrainment are negligible, (e) the tailwater depth is the temporal mean value of its fluctuations; the momentum equation can be used to derive the well-known Belanger's equation for the sequent depth ratio

$$\frac{y_{2*}}{y_1} = \frac{1}{2}\left[-1+\sqrt{1+8F_1^2}\right] \tag{2.1}$$

$$\frac{y_1}{y_{2*}} = \frac{1}{2}\left[-1+\sqrt{1+8F_2^2}\right] \tag{2.2}$$

where $F_1 = U_1/\sqrt{gy_1}$ and $F_2 = U_2/\sqrt{gy_2}$ are upstream and downstream Froude numbers with g being the acceleration due to gravity. The Froude numbers are an index of the free surface flow (Hager, 1995).

Equation (2.1) may be represented by the curve in Fig.2.2. This curve has been verified satisfactorily with many experimental data and has been found to be very useful in the analysis and design for hydraulic jumps (Chow, 1973).

For very small F_2, i.e. $F_2^2 \leq 0.05$ the following equation should be used (French, 1994):

$$\frac{y_1}{y_{2*}} = 2F_2^2 - 4F_2^4 + 16F_2^6 \tag{2.3}$$

For $F_1 > 2$, Eq. (2.1) may be approximated as (Hager, 1995):

$$\frac{y_{2*}}{y_1} = \sqrt{2}F_1 - \frac{1}{2} \tag{2.4}$$

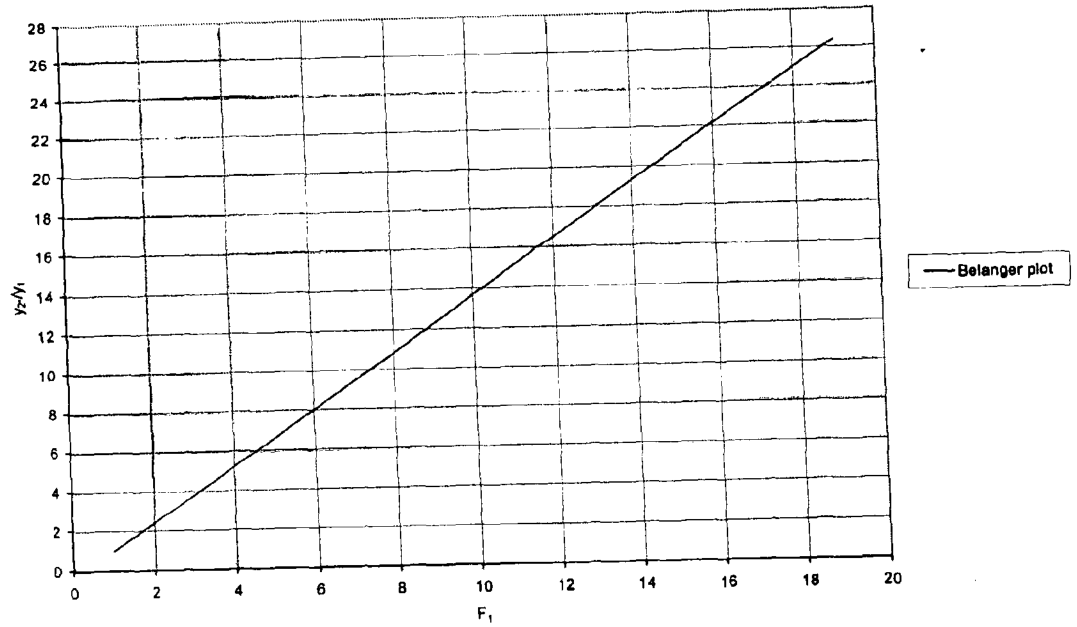

Fig.2.2 Plot between F_1 and y_{2*}/y_1 for hydraulic jump in a horizontal rectangular channel

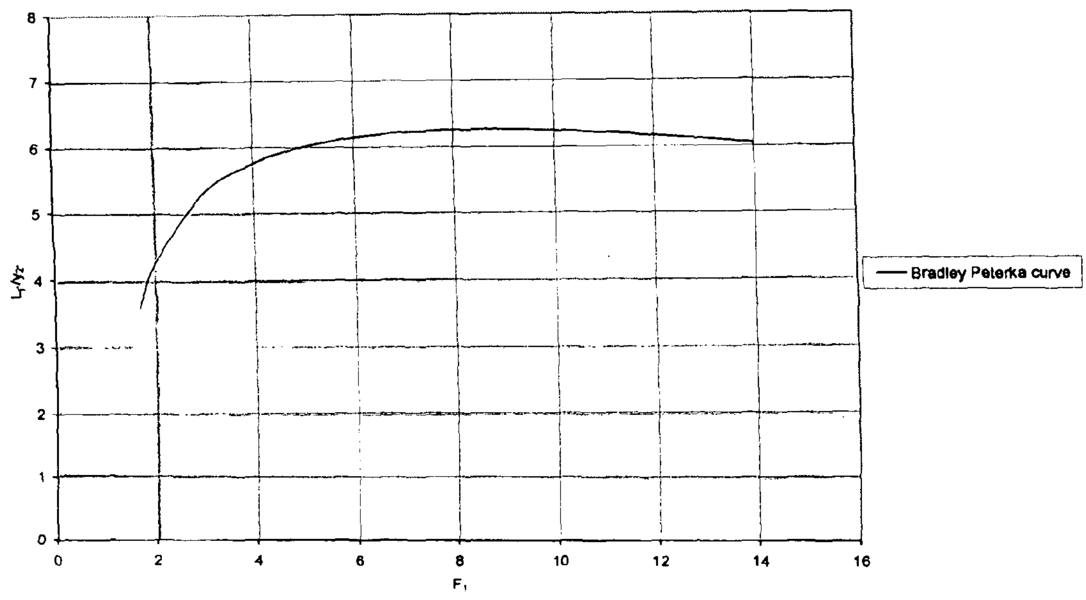

Figure 2.3 Length of the hydraulic jump on a horizontal floor

Thus, the sequent depths ratio is essentially proportional to F_1. For a given approach flow depth y_1, an increase of discharge thus yields a proportional increase of tailwater depth y_{2*}.

According to Hager and Bremen (1989), a scale-effect due to viscosity is negligible if the discharge is not too small. So for using Eq. (2.4), the discharge per unit width Q/b should be greater than 0.1 m^3/s.

A proper design of a jump-type stilling basin requires that the entire jump be contained within the basin at all discharges. This is possible only if the length of the jump L_{j*} can be predicted. The length of the jump is defined as the horizontal distance between the toe of the jump to a section where the water surface becomes essentially level after reaching the maximum depth. Some error in judgment in the estimation of length in hydraulic jump is to be expected because the downstream end of the jump cannot be located with a great degree of precision. The data on the length of the hydraulic jump generally show some scatter for this reason. One has to rely on considerable empiricism in predicting the length of the jump. Experimentally, it is found that $L_{j*}/y_{2*} = f\ (F_1)$. From the data of Bradley and Peterka (1957a),

$$\frac{L_{j*}}{y_1} = 10\alpha_j \tanh\left(\frac{F_1 - 1}{\alpha_j}\right) \tag{2.5}$$

with $\alpha_j = 22$. Using Eqs. (2.1) and (2.5) Bradley and Peterka have given the variation of L_{j*}/y_{2*} with F_1 as shown in Fig. 2.3. This curve is used in general. From the figure, it follows that while L_{j*}/y_{2*} depends on F_1 for small values of the inlet Froude number, at higher values (i.e., $F_1>5$) the relative jump length L_{j*}/y_{2*} is practically constant at a value of 6.2. For $4 < F_1 < 12$, a simple approximation to Eq. (2.5) is $L_{j*} = 6y_{2*}$. Elevatorski (1959) has given the following expression for the length of the jump,

$$L_{j*} = 6.9\ (y_{2*} - y_1) \tag{2.6}$$

The length of the surface roller is smaller than the length of the jump. The roller length increases from about $0.4L_{j*}$ at $F_1=3$ to about $0.7L_{j*}$ at $F_1=9$. Beyond the end of jump, the flow is practically not perturbed by the jump (Ranga Raju, 1993).

The free surface profile may vary as much as $0.2(y_{2*}-y_1)$.

The efficiency $\eta = \Delta H/H_1$ of the classical jump is equal to the mechanical head loss ΔH normalized by the approach energy head H_1. In terms of F_1,

$$\eta = \frac{\Delta H}{H_1} = \frac{8F_1^4 + 20F_1^2 - \left(8F_1^2 + 1\right)^{3/2} - 1}{8F_1^2\left(2 + F_1^2\right)} \tag{2.7}$$

Graphical solution for the sequent depths and energy dissipation is available in literature (French, 1994) for non-rectangular channels.

Recently Chaurasia (2003) has developed direct explicit equation for the pre-jump and post-jump depths and specific energy in a rectangular horizontal channel. These equations are given below,

$$y_1 = 0.196q^{0.98}\Delta H^{-0.47}\left[1 + 1.262q\Delta H^{-1.50}\right]^{-0.206} \tag{2.8}$$

$$y_2 = 1.0518q^{0.518}\Delta H^{0.223}\left[1 + 0.0476q^{2.667}\Delta H^{-4.0}\right]^{-0.221} \tag{2.9}$$

$$Ef_2 = 1.029q^{0.513}\Delta H^{0.223}\left[1 + 0.4329q^{0.733}\Delta H^{-1.10}\right]^{0.1631} \tag{2.10}$$

$$Ef_1 = Ef_2 + \Delta H \tag{2.11}$$

where Ef_1 and Ef_2 are the pre-jump and post-jump specific energies.

The above equations for hydraulic jump elements have very high accuracy and are applicable for a very wide range of values of discharge intensity and head loss without any limitations in comparison to other methods attempted so far.

2.3 Stabilization of Jump

If the tailwater depth is equal to the sequent depth y_2, corresponding to the given supercritical depth, the jump is formed at the toe of the structure. However, if the tailwater depth is larger (or smaller) than the required conjugate depth, the jump can be drowned (or repelled). In practice, one should anticipate a situation when the tailwater depth is not equal to the required conjugate depth at all discharges. Ideally, the jump should form close to the structure and certain appurtenances are used to control the location of jump, i.e., to force the jump to occur at a desired location. The jump is then known as a forced jump (Ranga Raju, 1993).

The hydraulic jump can be controlled or effected by sills of various designs, such as sharp-crested weir, broad-crested weir, abrupt rise and drop in channel floor. The sill ensures the formation of a jump and controls its position under all probable operating conditions. Beside sills, channel enlargement and contraction may also be resorted to for controlling the jump. Recent research on this subject has brought out the usefulness of the corrugated beds as an alternative method of jump stabilization. Various methods to control the jump are briefly discussed below (Chow, 1973).

2.3.1 Control by Sharp-crested Weir

Based on the analysis of experimental data, Forster and Skrinde have given a diagram shown in Fig. 2.4, depicting the relations among (a) Froude number F_1 of the approaching flow, (b) the ratio between the weir height h and the approaching depth y_1, and (c) the ratio between the distance X from the toe of the jump to the weir and the depth y_2 upstream from the weir. This diagram is used to analyze the effect of a given weir for known approach and tailwater conditions, provided that the normal tailwater depth y_3 does not affect the discharge over the weir crest; i.e., provided $y_3 < y_2 - 0.75h$.

If a point lies within the curves, jump will occur at a position indicated by interpolating for X/y_2. Points lying above and to the left of an interpolated curve represent the conditions when the weir is too high forcing the jump upstream and possibly drowning at the source. Points lying to the right of the curve represent the conditions under which the weir is too low, so that the jump is forced downstream, possibly washing out. For designing, curve $X/y_2 = 5$ should be used (Chow, 1973).

2.3.2 Control by Broad-crested Weir

For a broad-crested weir the relation between h/y_1 and F_1 is shown in Fig. 2.5. But, this curve may be used only if the downstream depth is lower than the critical depth on top of the weir, i. e., if $y_3 < (2y_2 + h)/3$, as the tailwater will not affect appreciably the relation between the head water elevation and the discharge. A broad-crested weir is advantageous to use as it has greater structural stability than a sharp-crested weir and usually requires low cost of excavation than an abrupt rise (Chow, 1973).

2.3.3 Control by Abrupt Rise and Drop

If the tailwater depth is less than the sequent depth corresponding to the subcritical flow depth, the steady location of the hydraulic jump within the stilling basin is obtained by means of the bottom rise. On the other hand if the downstream depth is more than the

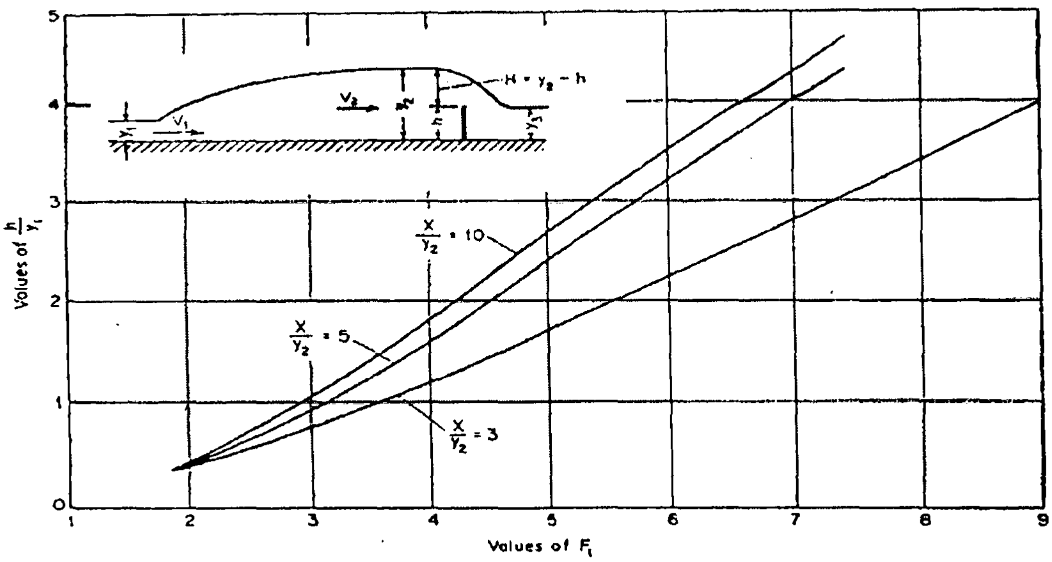

Fig. 2.4 Experimental relations among F_1, h/y_1 and X/y_2 for a sharp-crested weir

(After Forster and Skrinde)

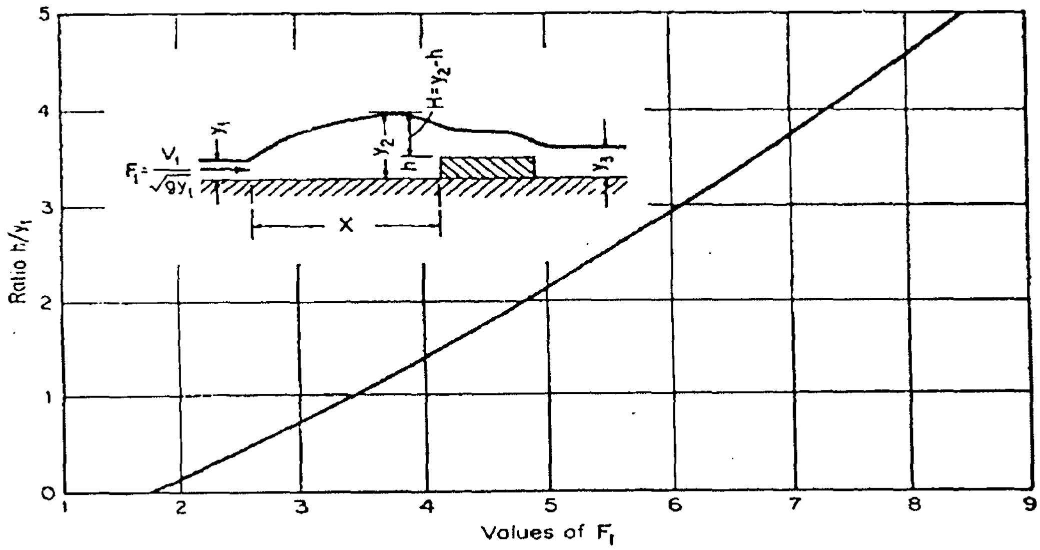

Fig. 2.5 Analytical relations between F_1 and h/y_1 for a broad-crested weir

(After Forster and Skirde)

sequent depth for a normal jump, a drop in the channel floor must be used in order to ensure a jump.

Depending on the tailwater depth, the locations of jump are different. A-jump is entirely located at the upstream zone of step and its roller ends just at the step. Lowering the tail water depth changes the A-jump to B-jump. The B-jump is defined as a jump at the down most position before it breaks into two distinct portions, namely a wave above the step and a downstream hydraulic jump. Depending on relative step size $S = s'/y_1$, s' being the rise or drop, the flow zone behind the step may be aerated or non-aerated. Regarding energy dissipation only A- and B-jumps are of interest, since the wave types yield supercritical flow at the downstream zone of the step.

A-jump is characterized by nearly hydrostatic pressure and uniform velocity distribution both at the toe of the jump and at the end of roller. If sequent depth ratio is represented as Y, for the case of abrupt rise the application of momentum equation in longitudinal direction of flow yields (Hager and Bretz, 1986):

$$F_1^2 = \frac{Y\left[(Y+S)^2 - 1\right]}{2(Y-1)} \tag{2.12}$$

By accounting properly for the pressure distribution at the step the corresponding relation for B-jump for abrupt rise is

$$F_1^2 = \frac{Y\left[(Y+S)^2 + S^2 - 1\right]}{2(Y-1)} \tag{2.13}$$

Similarly, for the case of abrupt drop, the sequent depth ratio for A-jump is given by

$$F_1^2 = \frac{Y\left[(Y-S)^2 - 1\right]}{2(Y-1)} \tag{2.14}$$

and for zero pressure on the step for B-jump

$$F_1^2 = \frac{Y\left[Y^2 - S^2 - 1\right]}{2(Y-1)} \tag{2.15}$$

2.3.4 Control by Channel Enlargement and Contraction

If the tailwater depth is larger than the sequent depth corresponding to the subcritical flow depth, the steady location of the hydraulic jump within the stilling basin can also be obtained by means of channel enlargement. On the other hand, if the downstream depth is smaller than the sequent depth for a normal jump, a contraction in the flow width can be used in order to ensure a jump.

For the case of gradual rectangular expanding channel the relation for the sequent depths in terms of the inflow Froude number F_1 and width ratio $\beta = B/b$, where B = downstream channel width, is given as (Hager, 1985):

$$F_1^2 = \frac{(\beta+1)(Y^2-1)\beta Y}{4(\beta Y-1)} \tag{2.16}$$

Asymptotically Eq. (2.16) may be simplified to

$$Y = \sqrt{\frac{2}{\beta+1}}\left(\sqrt{2}F_1 - \frac{1}{2}\right) \tag{2.17}$$

which always gives slightly lower values than Eq. (2.16).

For the case of abrupt enlargement, the following equation applies:

$$F_1^2 = \frac{\beta Y(\beta Y^2-1)}{2(\beta Y-1)} \tag{2.18}$$

Asymptotically Eq. (2.18) may be simplified to,

$$Y = \frac{1}{\beta}\left(\sqrt{2}F_1 - \frac{1}{2}\right) \tag{2.19}$$

Baffle blocks are used to control the hydraulic jump in stilling basins when there is deficiency of tailwater depth. The chute blocks are used to form a serrated device at the entrance to the stilling basin to assist in splitting and furrowing the incoming jet and lift a portion of it from the floor, producing a shorter length of jump. Baffle blocks dissipate energy by impact action. The end sill lifts the outgoing stream thereby controlling scour. The effect of these appurtenances is to shorten the stilling basin length to $2.7y_{2*}$ in USBR type II stilling basin as against $6.1y_{2*}$ required for a free hydraulic jump. Also, the minimum tailwater depth required is $0.83y_{2*}$ as against y_{2*} for an unaided jump.

2.3.5 Control by Corrugated Beds

The main concern with jumps on rough beds is that the roughness elements located in the upstream part of the stilling basin might be subjected to cavitation and possible erosion, resulting in the movement of the jump to the downstream unprotected streambed, thus causing erosion and endangering the structure itself. The study by Ead et. al. (2000) on turbulent open channel flow in circular corrugated culverts indicated that the intense mixing induced by the corrugations produced significant Reynolds shear stresses in the plane of the crests of the corrugations and significant reduction in the velocity field above the corrugations. It looked that, if jumps were made to occur on corrugated beds, significant reductions might occur in the required tailwater depth and length of the jumps. Further, if the crests of the corrugations were at the level of the upstream bed carrying the supercritical stream, the corrugations would not be protruding into the flow and, hence, may not be subjected to the same intensity of cavitation as in the case of protruding roughness.

Recently, an exploratory laboratory investigation was performed with hydraulic jumps on corrugated beds by Ead and Rajaratnam (2002) for relative roughness t/y_1 values of 0.50, 0.43 and 0.25 with Froude numbers ranging from 4 to 10. Figure 2.6 shows a definition sketch for free jumps on corrugated beds. The tailwater depth required to form a jump was found to be noticeably smaller than that for the corresponding jumps on smooth beds. The tailwater depth required to form jump on corrugated beds was found to be reduced to three-fourths of that on smooth bed. Also, the length of the jumps was about half of those on smooth beds. The integrated bed shear stress on the corrugated bed was about ten times that on smooth beds. The results of the study showed that the idea of using corrugated beds for energy dissipation below hydraulic structures is a good one and needs much attention.

Rahul (2003) at IIT Roorkee has validated the results of Ead and Rajaratnam (2002) by conducting experiments of hydraulic jump on corrugated bed at three values of relative roughnesses 0.20, 0.43, and 0.70 of the bed.

2.4 Concluding Remarks

Various methods to stabilize the jumps have been discussed in this chapter. It is seen that if the downstream depth is more than the sequent depth for a normal jump, one goes for abrupt drop or channel enlargement. On the other hand, if the downstream depth is inadequate for the jump to form, the options are rise in bed level and baffle blocks. Also, the option of corrugated beds is being explored to reduce the downstream depth requirement to form a jump.

During the review it was found that the study on corrugated beds needed much attention and with a view to carry forward the previous work the objectives were set for the present study. Broadly speaking, the study of the effects of the dimensions of the corrugated sheet on various parameters of the jump was set as the main objective.

Chapter3

EXPERIMENTAL PROGRAMME

3.1 General

This chapter describes the experimental work carried out for the present study. Experiments were conducted in the Hydraulic Laboratory of the Department of Civil Engineering Department at IIT Roorkee. First experiments were performed on smooth bed for different discharges under different gate openings. Then fabricated corrugated sheets were placed in the flume and the experiments were performed on them for the same discharges and same gate openings as those used for the smooth bed.

3.2 Experimental Set-up

The experiments were conducted on a rectangular flume 0.3m wide, 0.8m deep and 5.0m long. The flume was framed with side glass wall. The bed surface was smooth with a cement plaster. The flume had two gates, one at the inlet end and the other one i.e., the tailgate was provided just before the end of the flume. Water entered the flume under the sluice gate with a streamlined lip, thereby producing a uniform supercritical stream with a thickness of y_1. The tailgate was used to control the tailwater depth in the flume. Fig. 3.1 shows the sketch of the experimental set-up. The flume is equipped with circular pipe rails (parallel to the bed) to hold movable instrument platforms for mounting point gauges. A triangular notch was provided at downstream of the tailgate to measure the discharge in the flume. A constant head tank was used to cause flow of water into the flume, discharge being controlled through a valve. Corrugated G.I./PVC sheets were nailed on the bed of the flume in such a way that the crests of corrugations were at the same level as the upstream bed on which the supercritical stream was produced by the sluice gate (Photograph 3.1). The sheet was fixed over the full width of the flume for a length of 105cm. The corrugations acted as depressions in the bed, to create a system of turbulent eddies which might increase the bed shear stresses. Eight corrugated sheets, with nearly sinusoidal corrugations of wavelength s perpendicular to the flow direction, and amplitude t were used for the study. The details of the sheets are shown in Table 3.1.

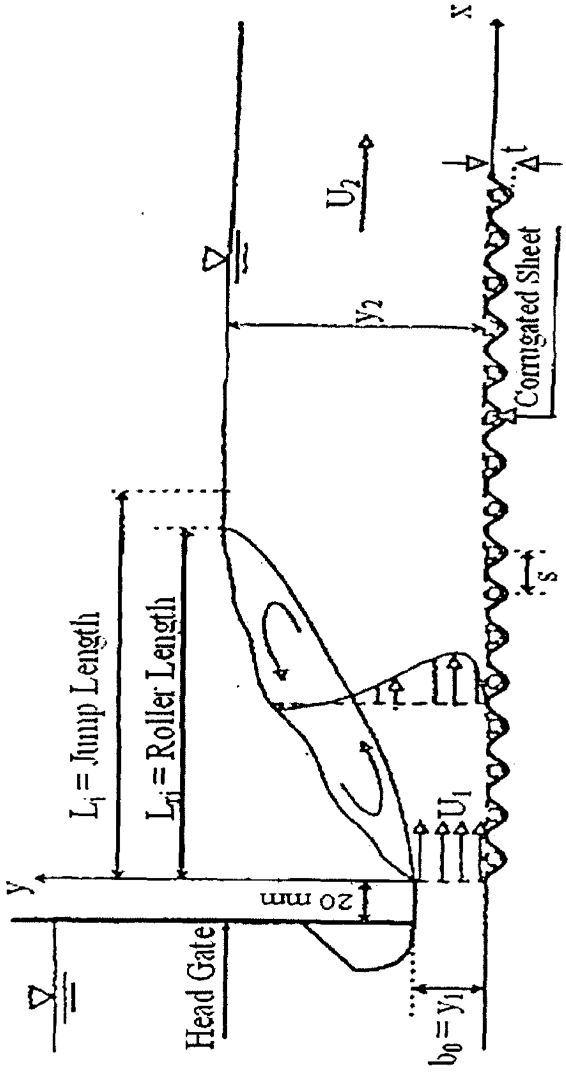

Fig. 2.6 Definition Sketch of Hydraulic Jump on Corrugated Beds (*After Ead and Rajaratnam, 2002*)

discharge in the flume. A constant head tank was used to cause flow of wate... ..... flume, discharge being controlled through a valve. Corrugated G.I./PVC sheets were nailed on the bed of the flume in such a way that the crests of corrugations were at the same level as the upstream bed on which the supercritical stream was produced by the sluice gate (Photograph 3.1). The sheet was fixed over the full width of the flume for a length of 105cm. The corrugations acted as depressions in the bed, to create a system of turbulent eddies which might increase the bed shear stresses. Eight corrugated sheets, with nearly sinusoidal corrugations of wavelength s perpendicular to the flow direction, and amplitude t were used for the study. The details of the sheets are shown in Table 3.1.

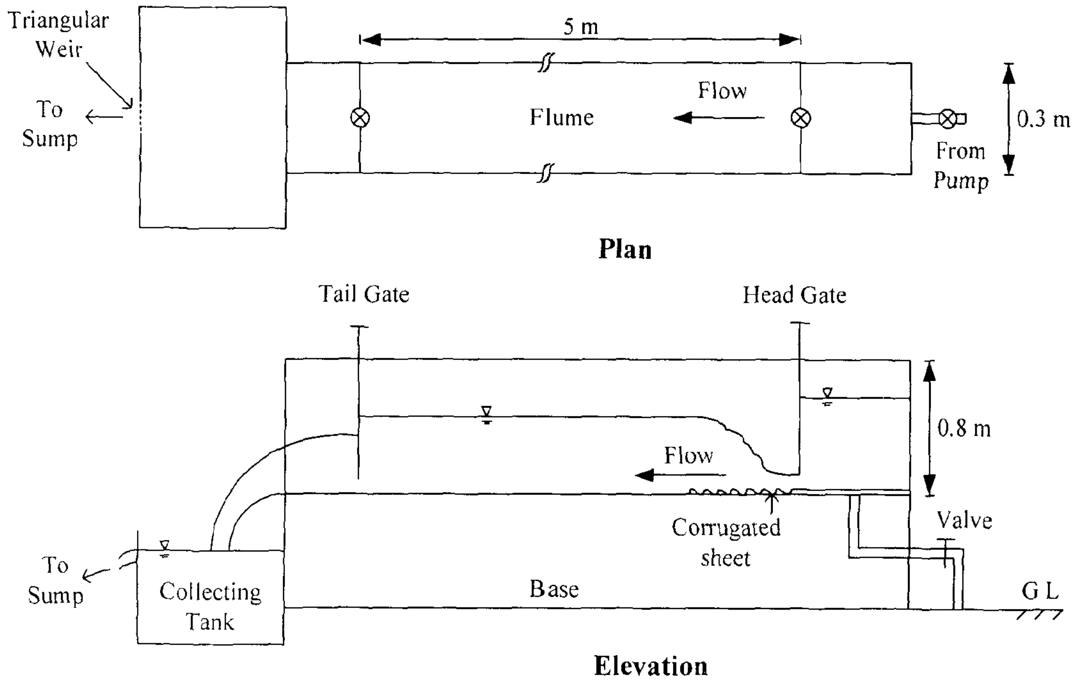

Fig. 3.1 Sketch of Experimental Set-up

Table 3.1 Details of Corrugated sheets

Sheet no.	Amplitude (t mm)	Wavelength (s mm)
1.	15	75
2.	20	50
3.	20	60
4.	25	62
5.	25	75
6.	25	100
7.	25	125
8.	35	140

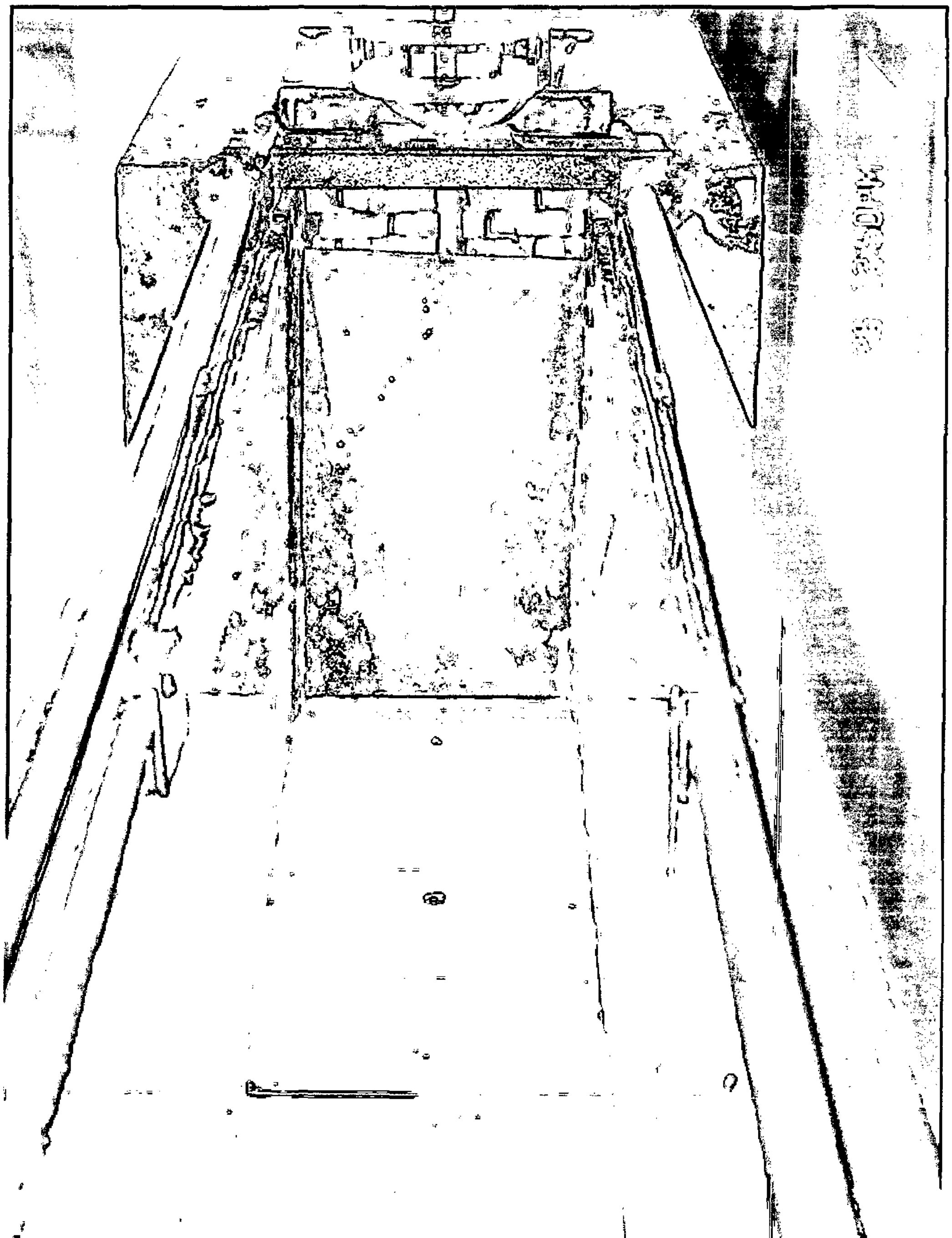

Photograph 3.1 Corrugated sheet placed on the flume bed

Photograph 3.2 Hydraulic Jump on Corrugated bed in a flume

3.3 Experimental Procedure

Hydraulic jumps were produced on the smooth horizontal bed for three different discharges for every gate opening. The tailgate was adjusted such that the hydraulic jump will form at 20mm downstream of the upstream gate. The upstream gate opening (y_1) for the jump on the smooth as well as on the corrugated bed was adjusted according to the designed relative roughness (for jump on corrugated bed) of 0.55, 0.60, 0.65, 0.7 and 0.75. For the measurement of the discharges, a triangular notch was provided at downstream of the tailgate. Measurements of the depth of the water-flow were made in the vertical centerline plane of the flume. Although, the measurements of the length of the jumps were made up to the point where the depth becomes constant, still the accuracy involved was based on the judgment of the observer.

The jumps on corrugated bed were performed with PVC/G.I. corrugated sheets placed on the bed of the flume such that the crests of the corrugations were at the level of the upstream bed carrying the supercritical flow and subcritical flow (Photograph 3.2). Hydraulic jumps are formed for three different discharges corresponding to each gate opening. Experiments were performed for five different gate openings, giving a set of fifteen readings for each sheet. Eight sheets having different combinations of s and t are used. The discharge as well as the inlet gate opening for the experiment on smooth bed as well as on the rough bed was kept the same. No corrections were made to account for turbulence. The Reynolds number $R_1=\rho U_1 y_1/\upsilon$ was in the range of 47936-93000. Five values of the relative roughness, defined as the ratio of the amplitude of the corrugations to the supercritical depth just before the jump, t/y_1 of 0.55, 0.60, 0.65, 0.70, and 0.75 were used. The value of s/y_1 ranges from 1.36 to 3.75.

3.4 Data Collection

The data collected during the present experimental study are furnished in Appendix-I. The data of the study of Ead and Rajaratnam (2002) are presented in Appendix-II while the data of Rahul (2003) are given in Appendix-III.

The range of different parameters used for analysis in the present study along with those of the previous studies are presented in Table 3.2.

Table 3.2 Range of Data for different studies

Parameter	Present study	Ead and Rajaratnam	Rahul
Amplitude t (mm)	15-35	13-22	15
Wavelength s (mm)	60-140	68	75
Pre-jump depth y_1 (cm)	2 to 6.36	2.54 to 5.08	2.17 to 7.5
Discharge intensity q ($m^3/s/m$)	0.048 to 0.093	0.051 to 0.207	0.042 to 0.164
Post-jump depth y_2 (cm)	0.098 to 0.142	0.104 to 0.310	0.116 to 0.186
Length of jump (m)	0.37 to 0.62	0.41 to 1.29	0.44 to 0.58

3.5 Concluding Remarks

In this chapter, the details of the experimental set-up and procedure along with the details of the data collected were summarized. The data used in the present study offers a wide range of values. Next the entire composite data of all the studies is to be analyzed to obtain the results.

Chapter4

ANALYSIS OF DATA

4.1 General

First of all dimensional analysis is performed using Buckingham's Pi-Theorem to find out the functional relationship for the tailwater depth and length of the jump on corrugated beds. Thereafter, verification of Belanger's equation has been done for the observed data of smooth bed. Then, the data collected in the present study have been analyzed along with the data of Ead and Rajaratnam (2002) and Rahul (2003) and the results relating to the tailwater depth, the length of the jump and the integrated shear stress have been discussed in this chapter.

4.2 Dimensional Analysis

For a jump on smooth bed with supercritical depth y_1 and mean velocity U_1, the depth at the end of the jump y_{2*} may be written as

$$y_{2*} = f_1 (y_1, U_1, g, \rho, \mu) \tag{4.1}$$

where ρ = mass density and μ = dynamic viscosity of the fluid.

From Belanger's equation it is known that,

$$\frac{y_{2*}}{y_1} = f_2(F_1) \tag{4.2}$$

For a jump on a corrugated bed, the bed characteristics, that is, corrugation amplitude t and wavelength s, are also supposed to influence the depth at the end of the jump y_2 besides y_1 and U_1 and, hence, one may write,

$$y_2 = f_3 (y_1, U_1, g, \rho, \mu, t, s) \tag{4.3}$$

Using the Pi theorem, it can be shown that

$$\frac{y_2}{y_1} = f_4\left(F_1 = \frac{U_1}{\sqrt{gy_1}}, R_1 = \frac{\rho U_1 y_1}{\mu}, \frac{t}{y_1}, \frac{s}{y_1}\right) \tag{4.4}$$

For large values of the Reynolds number (involved in this study), viscous effects may be neglected (Rajaratnam 1976; Hager and Bremen 1989) and Eq. (4.4) reduces to

$$\frac{y_2}{y_1} = f_5\left(F_1, \frac{t}{y_1}, \frac{s}{y_1}\right) \tag{4.5}$$

Using Eq. (4.2) one can rewrite Eq. (4.5) as

$$\frac{y_2}{y_1} = f_6\left(\frac{y_{2*}}{y_1}, \frac{t}{y_1}, \frac{s}{y_1}\right) \tag{4.6}$$

Or

$$\frac{y_{2*} - y_2}{y_{2*}} = f_7\left(\frac{t}{y_1}, \frac{s}{y_1}\right) \tag{4.7}$$

Performing a similar dimensional analysis for the length of the jump on corrugated beds yields,

$$\frac{L_{j*} - L_j}{L_j} = f_8\left(\frac{t}{y_1}, \frac{s}{y_1}\right) \tag{4.8}$$

4.3 Verification of Belanger's Equation

First the data obtained for the tailwater depth for smooth beds are verified with the Belanger's equation to check the consistency of the data observed. As Belanger's equation give conservative values, so actual data points in Fig. 4.1 should lie below the line obeying the Belanger's equation. But, one finds that the observed data for smooth bed very nearly satisfy the Belanger's equation (in fact, for higher Froude number, the data points lie above the line). Although this signifies some error in the observations still one can use the smooth bed data for the analysis as the error will be small.

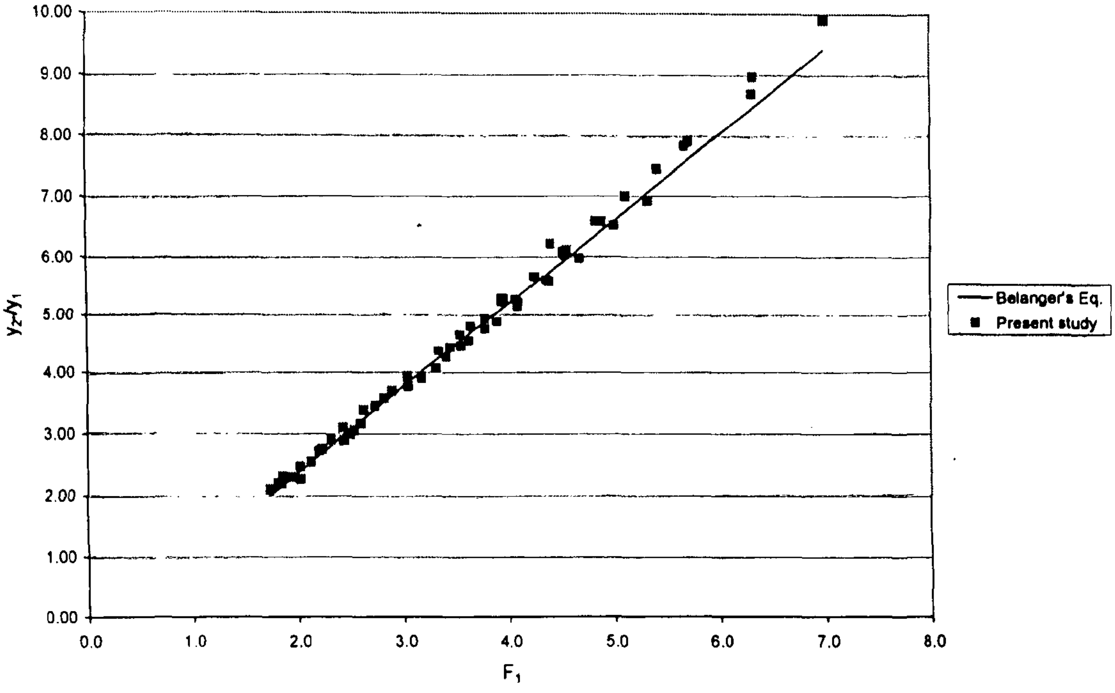

Figure 4.1 Verification of Belanger's Equation

4.4 Tailwater depth for hydraulic jump on corrugated bed

To see the effect of the amplitude and wavelength of the corrugations on the tailwater depth, two graphs were plotted. The first between $(y_{2*}-y_2)/y_{2*}$ and t/y_1 for three different range of s/y_1, 1 to 2, 2 to 3, 3 to 4. The second one is plotted between $(y_{2*}-y_2)/y_{2*}$ and s/y_1 for different values of t/y_1. For both these plots, entire composite data of the present study and those of Ead and Rajaratnam (2002) and Rahul (2003) have been used.

From the plots, one finds that, for the range of data studied here, the amplitude and the wavelength do not affect the tailwater depth. In the study of Ead also, the tailwater depth was shown to be independent of the relative roughness. This is so because the crests of the corrugations being at the level of the upstream bed level, the corrugations act more like cavities and, hence, the channel bed roughness is almost constant. Further, from both the graphs Fig. 4.2 (a) and (b) it can be shown that,

$$\frac{y_{2*}-y_2}{y_{2*}} = 0.24 \tag{4.9}$$

Or,

$$y_2 = 0.76 y_{2*} \tag{4.10}$$

Substituting for y_{2*} from Eq. (2.1),

$$\frac{y_2}{y_1} = \frac{0.76}{2}\left(-1+\sqrt{1+8F_1^2}\right) \tag{4.11}$$

From Fig. 4.3 one finds that Eq. (4.11) reduces to

$$\frac{y_2}{y_1} \cong F_1 \tag{4.12}$$

Hence, the tailwater depth required to form a jump with corrugated beds was found to be nearly 76% of that required on smooth beds. This emphasizes the usefulness of the corrugated beds when the tailwater depth is not adequate.

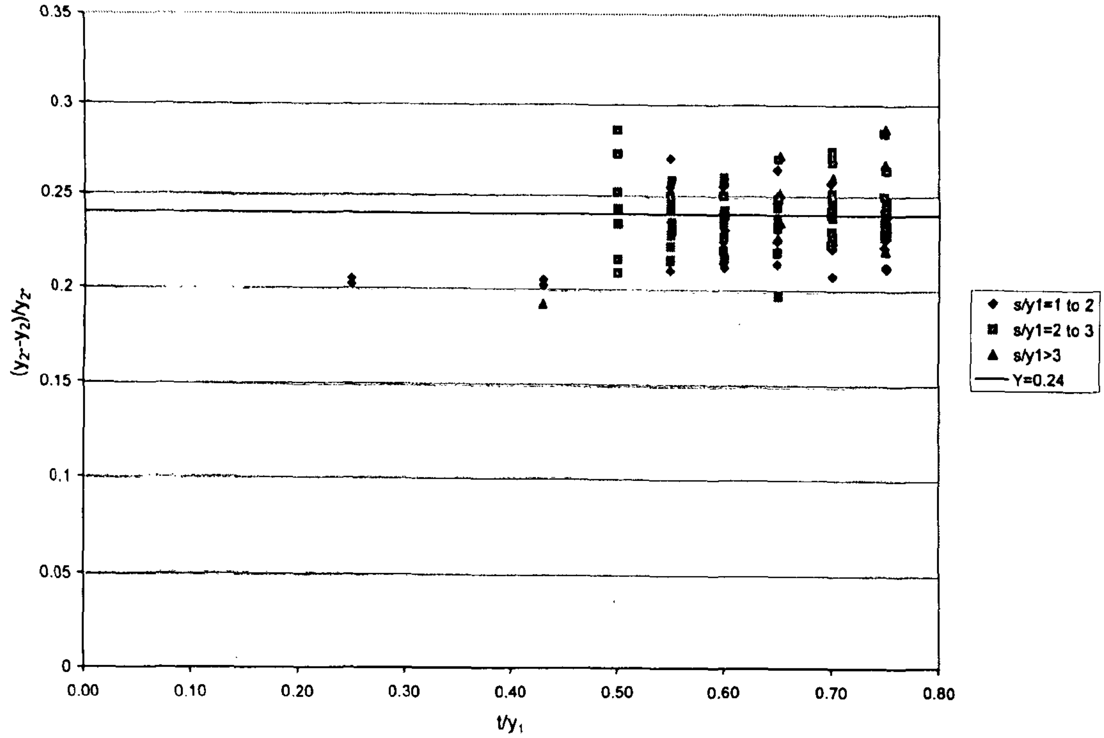

Figure 4.2(a) Variation of $(y_{2*}-y_2)/y_{2*}$ with t/y_1 for different range of s/y_1

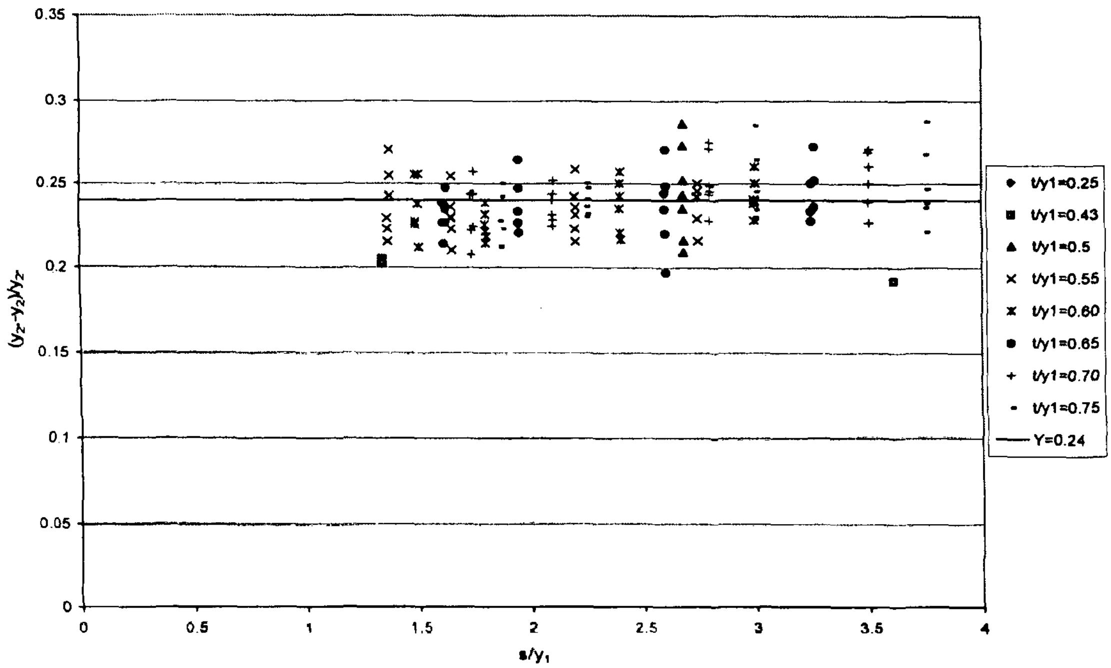

Figure 4.2(b) Variation of $(y_{2*}-y_2)/y_{2*}$ with s/y_1 for different t/y_1

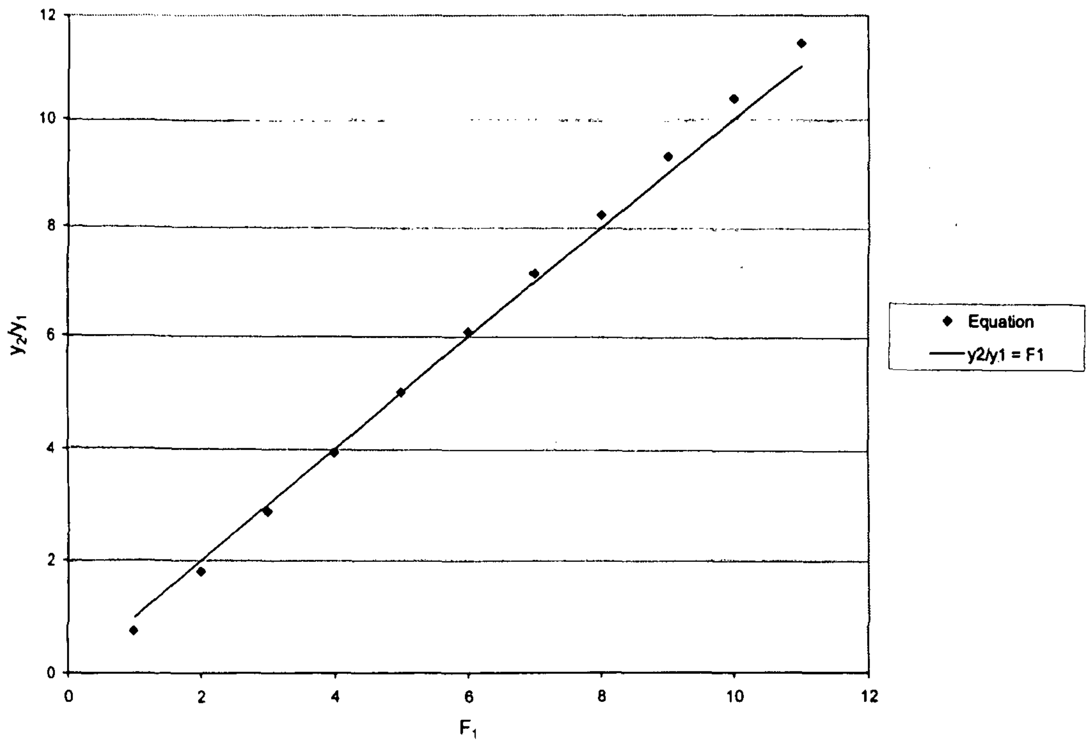

Figure 4.3 Comparison of derived equation with linear plot between y_2/y_1 and F_1

4.5 Length of hydraulic jump on corrugated bed

First, the data for normalized length of the jump, L_j/y_{2*} on smooth beds were plotted with Froude number. This was found to follow Bradley-Peterka curve for the length of the hydraulic jump on a horizontal smooth floor. From the plot, it was found that while L_j/y_{2*} depends on F_1 for small values of the inlet Froude number, at higher values (F_1>5) the relative jump length L_j/y_{2*} becomes practically constant at a value of 6.1. Next, plot for the relative jump length L_j/y_{2*} on corrugated beds is prepared. From Fig. 4.4, it can be concluded that the length of the jump on corrugated beds is independent of the Froude number and is nearly thrice of the tailwater depth from the Belanger's equation,

$$\frac{L_j}{y_{2*}} \cong 3 \qquad (4.13)$$

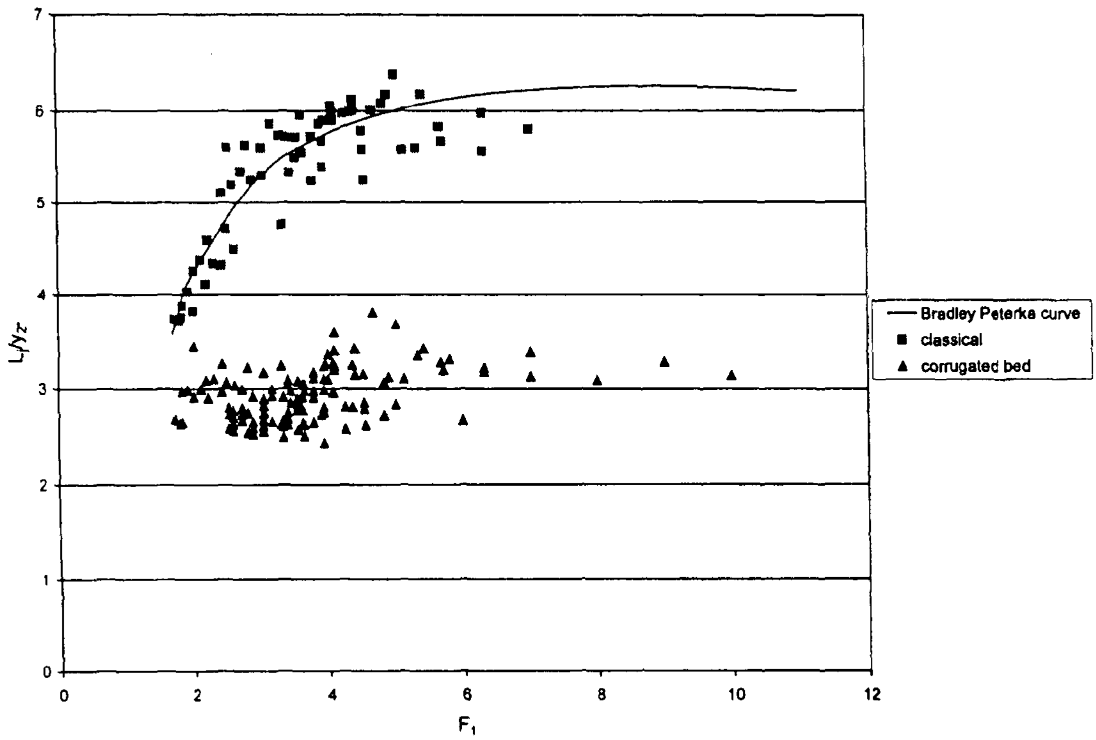

Figure 4.4 Variation with F_1 of normalized length of jump L_j/y_{2*}

4.6 Shear stress under hydraulic jump on corrugated bed

The reason attributed for the small downstream depth y_2 of these jumps on corrugated beds is the existence of increased bed shear stresses. If F_τ is the integrated bed shear stress on the horizontal plane coinciding with the crests of the corrugations, it can be found using the integral momentum equation

$$F_\tau = (P_1 - P_2) + (M_1 - M_2) \tag{4.14}$$

Where P_1, P_2 and M_1, M_2 = integrated pressures and momentum fluxes at the sections just before and after the jump. Using the relation $F_\tau = \varepsilon_1 M_1$, Eq. (4.14) can be reduced to the form (Ead and Rajaratnam, 2002),

$$\left(\frac{y_2}{y_1}\right)^3 - \left(1 + 2F_1^2 - 2\varepsilon_1 F_1^2\right)\left(\frac{y_2}{y_1}\right) + 2F_1^2 = 0 \tag{4.15}$$

Equation (4.15) reduces to the Belanger's equation when the shear force on the bed is neglected. Substituting Eq. (4.12) in Eq. (4.15), one obtains,

$$\varepsilon_1 = \frac{(F_1 - 1)^2}{2F_1^2} \tag{4.16}$$

The shear force coefficient introduced by Rajaratnam (1965) was defined as $\varepsilon = F_\tau / \rho g y_1^2/2$. Using Eqs. (4.12) and (4.14), it can be shown that (Ead and Rajaratnam, 2002)

$$\varepsilon = \varepsilon_1 2F_1^2 = (F_1 - 1)^2 \tag{4.17}$$

Using $F_\tau = \varepsilon P_1$ in Eq. (4.14), it can be shown that (Ead and Rajaratnam, 2002)

$$\varepsilon = \left[1 - \left(\frac{y_2}{y_1}\right)^2\right] + 2q^2\left(\frac{y_2 - y_1}{g y_1^3 y_2}\right) \tag{4.18}$$

Rajaratnam (1965) has shown that for jumps on smooth bed shear force coefficient ε is very small and increases slowly to attain a maximum value of 9 at Froude number 10. In contrast, one finds from Fig. 4.5 that for jumps on corrugated beds, ε increases exponentially attaining a high value of 75 at Froude number 10. The trendline following the present analysis is given as,

$$\varepsilon = 0.92F_1^2 - 1.74F_1 + 1.32 \tag{4.19}$$

This validates the findings behind the decreased tailwater requirements in corrugated beds as the decrease is, obviously, a result of the increased bed shear stress.

This validates the findings behind the decreased tailwater requirements in corrugated beds as the decrease is, obviously, a result of the increased bed shear stress.

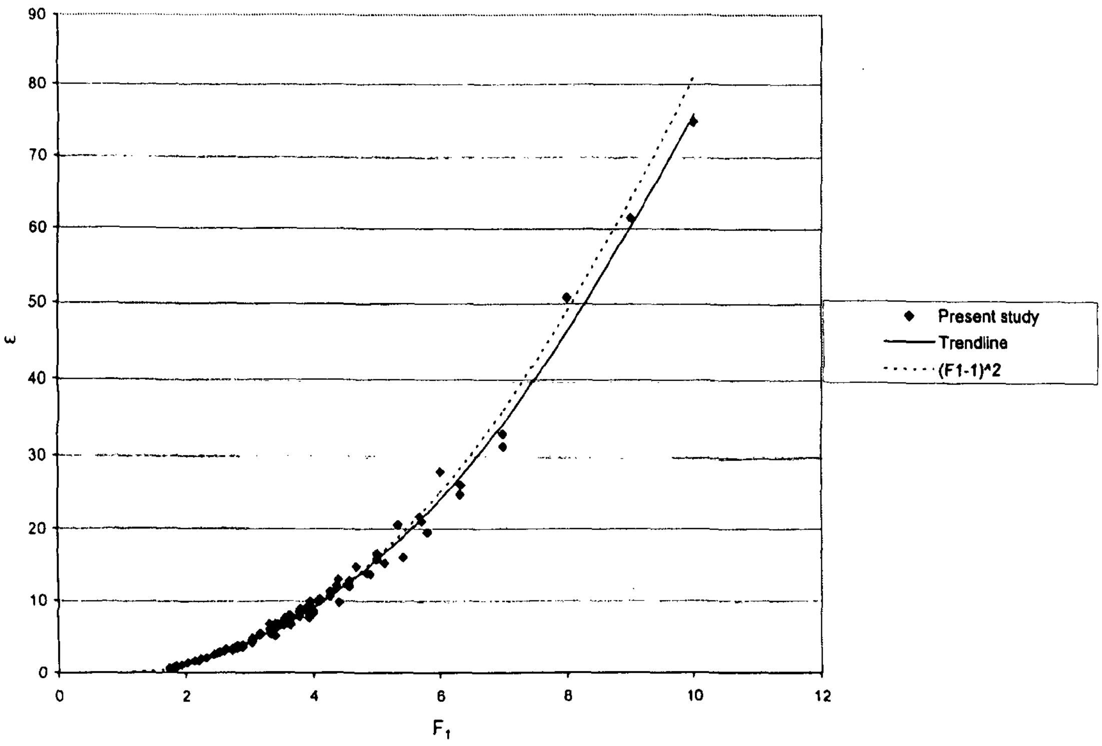

Figure 4.5 Variation of shear force coefficient with Froude number

Suggestions-

1. Before this idea can be used in practice, it would be useful to carry out further investigations to evaluate the effect of s/y_1 over a still larger range.

2. Further, the idea of using a configuration such that the crests of the corrugations are partially below the upstream bed level and partially protruding into the flow should also be explored, where the corrugations may not be subjected to the same intensity of cavitation as in the case of fully protruding roughness and still one may expect a fruitful reduction in the tailwater depth.

18. Bidone, Giorgio, "Observations on the height of the hydraulic jump in 1818-a report." (as referred in 10).
19. Belanger, J.B., "Essay on the Numerical Solution of some problems relative to the steady flow of water," Paris, 1828 (as referred in 10).
20. Darcy, H. and Bazin, H., "Experimental research on backwater and wave propagation," Hydraulic Researches-Vol.II, Paris, 1865 (as referred in 10).
21. Safranez, Kurt, "Hydraulic Jump and energy dissipation of water," Der Bauingenieur, Berlin, vol.8 (as referred in 10).
22. Forster, John W. and Skrinde, Raymond A., "Control of the hydraulic jump by sills," Transactions, American Society of Civil Engineers, Vol.115, pp.973-987, 1950 (as referred in 10).
23. Bradley, J.N. and Peterka, A.J., "The hydraulic design of stilling basins, hydraulic jumps on a horizontal apron," Journal of Hydraulic Division, Proc. ASCE, Paper No. 1401, October 1957, pp. 1401-1-25 (as referred in 15).
24. Research studies on stilling basins, energy dissipators, and associated appurtenances, U.S. Bureau of Reclamation, Hydraulic Laboratory Report No. Hyd-399, June 1, 1955 (as referred in 10).
25. McCorquodale, J. A. (1986), "Chapter 8: Hydraulic jumps and internal flows," Encyclopedia of fluid mechanics, N.P. Cheremisinoff, ed., Vol.2, Gulf Publishing, Houston, 120-173 (as referred in 10).
26. Leutheusser, H.J. and Kartha, V. C., "Effects of inflow condition on hydraulic jump," Journal of the Hydraulics Division, ASCE, Vol. 98, No. HY8, Proc. Paper 9088, Aug. 1972, pp. 1367-1385.
27. Leutheusser, H.J. and Schiller, Eric J., "Hydraulic Jump in a Rough Channel," Water Power and Dam Construction, Vol.27, No.5, May 1975, pp. 186-191.

DETAILS OF DATA

y_{2*} = tailwater depth on smooth bed

y_2 = tailwater depth on corrugated bed

L_{rj} = length of roller on corrugated bed

L_j = length of jump on corrugated bed

L_{j*} = length of jump on smooth bed

q = discharge intensity = discharge per unit width of flume

F_1 = Froude number = $\frac{U_1}{\sqrt{gy_1}}$

R_1 = Reynolds number = $\frac{\rho U_1 y_1}{\upsilon}$

ε = shear force coefficient = $\frac{F_\tau}{\rho g y_1^2 / 2}$

APPENDIX - I

t	s	y_1	q	y_{2^*}	y_2	L_{j^*}	L_{rj}	L_j	t/y_1	s/y_1	U_1	F_1	R_1	$(y_{2^*}-y_2)/y_{2^*}$	L_j/y_{2^*}	y_2/y_1	ε
(mm)	(mm)	(cm)	($m^3/s/m$)	(m)	(m)	(m)	(m)	(m)			(m/s)						
15	75	2.73	0.066	0.163	0.123	0.98	0.43	0.62	0.55	2.75	2.42	4.7	66000	0.245	3.80	4.51	14.661
15	75	2.73	0.062	0.152	0.114	0.93	0.38	0.52	0.55	2.75	2.27	4.4	62000	0.250	3.42	4.18	12.856
15	75	2.73	0.056	0.144	0.111	0.85	0.33	0.47	0.55	2.75	2.05	4.0	56000	0.229	3.26	4.07	8.163
15	75	2.50	0.066	0.173	0.128	0.97	0.45	0.58	0.60	3.00	2.64	5.3	66000	0.260	3.35	5.12	20.521
15	75	2.50	0.062	0.163	0.124	1.04	0.41	0.60	0.60	3.00	2.48	5.0	62000	0.239	3.68	4.96	16.442
15	75	2.50	0.056	0.152	0.114	0.88	0.35	0.48	0.60	3.00	2.24	4.5	56000	0.250	3.16	4.56	12.151
15	75	2.30	0.062	0.180	0.131	1.05	0.43	0.59	0.65	3.26	2.70	5.7	62000	0.272	3.28	5.70	21.662
15	75	2.30	0.056	0.161	0.123	0.90	0.37	0.50	0.65	3.26	2.43	5.1	56000	0.236	3.11	5.35	15.122
15	75	2.30	0.048	0.143	0.107	0.86	0.34	0.45	0.65	3.26	2.09	4.4	48000	0.252	3.15	4.65	9.665
15	75	2.14	0.062	0.192	0.140	1.02	0.44	0.61	0.70	3.50	2.90	6.3	62000	0.271	3.18	6.54	25.944
15	75	2.14	0.056	0.169	0.125	0.96	0.40	0.54	0.70	3.50	2.62	5.7	56000	0.260	3.20	5.84	20.950
15	75	2.14	0.048	0.141	0.109	0.87	0.31	0.44	0.70	3.50	2.24	4.9	48000	0.227	3.12	5.09	13.576
15	75	2.00	0.062	0.198	0.145	1.15	0.49	0.67	0.75	3.75	3.10	7.0	62000	0.268	3.38	7.25	32.887
15	75	2.00	0.056	0.174	0.133	1.04	0.41	0.56	0.75	3.75	2.80	6.3	56000	0.236	3.22	6.65	24.678
15	75	2.00	0.048	0.149	0.116	0.92	0.34	0.51	0.75	3.75	2.40	5.4	48000	0.221	3.42	5.80	15.952
20	50	3.64	0.077	0.169	0.128	0.93	0.27	0.47	0.55	1.37	2.12	3.5	77000	0.243	2.78	3.52	6.570
20	50	3.64	0.075	0.161	0.120	0.86	0.30	0.48	0.55	1.37	2.06	3.4	75000	0.255	2.98	3.30	6.697
20	50	3.64	0.072	0.148	0.108	0.85	0.31	0.48	0.55	1.37	1.98	3.3	72000	0.270	3.24	2.97	6.725
20	50	3.33	0.075	0.176	0.131	1.00	0.35	0.57	0.60	1.50	2.25	3.9	75000	0.256	3.24	3.93	8.686
20	50	3.33	0.072	0.164	0.125	0.94	0.32	0.52	0.60	1.50	2.16	3.8	72000	0.238	3.17	3.75	7.906
20	50	3.33	0.069	0.151	0.119	0.84	0.32	0.46	0.60	1.50	2.07	3.6	69000	0.212	3.05	3.57	7.160
20	50	3.08	0.072	0.174	0.131	1.04	0.38	0.49	0.65	1.62	2.34	4.3	72000	0.247	2.82	4.25	10.577
20	50	3.08	0.069	0.162	0.124	0.98	0.35	0.53	0.65	1.62	2.24	4.1	69000	0.235	3.27	4.03	9.761
20	50	3.08	0.066	0.150	0.116	0.88	0.30	0.41	0.65	1.62	2.14	3.9	66000	0.227	2.73	3.77	9.140
20	50	2.86	0.069	0.175	0.130	0.92	0.34	0.46	0.70	1.75	2.41	4.6	69000	0.257	2.63	4.55	12.702
20	50	2.86	0.066	0.160	0.121	0.96	0.33	0.45	0.70	1.75	2.31	4.4	66000	0.244	2.81	4.23	12.090
20	50	2.86	0.062	0.147	0.114	0.88	0.39	0.50	0.70	1.75	2.17	4.1	62000	0.224	3.40	3.99	10.207
20	50	2.67	0.066	0.176	0.132	1.07	0.40	0.54	0.75	1.87	2.47	4.8	66000	0.250	3.07	4.94	13.778
20	50	2.67	0.062	0.161	0.122	0.90	0.34	0.46	0.75	1.87	2.32	4.5	62000	0.242	2.86	4.57	12.284
20	50	2.67	0.056	0.139	0.108	0.82	0.33	0.45	0.75	1.87	2.10	4.1	56000	0.223	3.24	4.04	9.924
20	60	3.64	0.077	0.169	0.126	0.93	0.34	0.49	0.55	1.65	2.12	3.5	77000	0.254	2.90	3.46	6.841

t	s	y_1	q	y_{2*}	y_2	L_{j*}	L_{rj}	L_j	t/y_1	s/y_1	U_1	F_1	R_1	$(y_{2*}-y_2)/y_{2*}$	L_j/y_{2*}	y_2/y_1	ε
(mm)	(mm)	(cm)	(m^3/s/m)	(m)	(m)	(m)	(m)	(m)			(m/s)						
20	60	3.64	0.075	0.161	0.123	0.86	0.35	0.46	0.55	1.65	2.06	3.4	75000	0.236	2.86	3.38	6.323
20	60	3.64	0.072	0.148	0.115	0.85	0.26	0.39	0.55	1.65	1.98	3.3	72000	0.223	2.64	3.16	5.996
20	60	3.33	0.075	0.176	0.134	1.00	0.31	0.43	0.60	1.80	2.25	3.9	75000	0.239	2.44	4.02	8.146
20	60	3.33	0.072	0.164	0.126	0.94	0.33	0.51	0.60	1.80	2.16	3.8	72000	0.232	3.11	3.78	7.740
20	60	3.33	0.069	0.151	0.118	0.84	0.29	0.42	0.60	1.80	2.07	3.6	69000	0.219	2.78	3.54	7.311
20	60	3.08	0.072	0.174	0.128	1.04	0.34	0.45	0.65	1.95	2.34	4.3	72000	0.264	2.59	4.16	11.197
20	60	3.08	0.069	0.162	0.122	0.98	0.32	0.48	0.65	1.95	2.24	4.1	69000	0.247	2.96	3.96	10.144
20	60	3.08	0.066	0.150	0.116	0.88	0.30	0.41	0.65	1.95	2.14	3.9	66000	0.227	2.73	3.77	9.140
20	60	2.86	0.069	0.175	0.133	0.92	0.35	0.46	0.70	2.10	2.41	4.6	69000	0.240	2.63	4.65	11.944
20	60	2.86	0.066	0.160	0.123	0.96	0.37	0.52	0.70	2.10	2.31	4.4	66000	0.231	3.25	4.30	11.639
20	60	2.86	0.062	0.147	0.114	0.88	0.31	0.47	0.70	2.10	2.17	4.1	62000	0.224	3.20	3.99	10.207
20	60	2.67	0.066	0.176	0.132	1.07	0.35	0.48	0.75	2.25	2.47	4.8	66000	0.250	2.73	4.94	13.778
20	60	2.67	0.062	0.161	0.123	0.90	0.32	0.45	0.75	2.25	2.32	4.5	62000	0.236	2.80	4.61	12.013
20	60	2.67	0.056	0.139	0.107	0.82	0.34	0.50	0.75	2.25	2.10	4.1	56000	0.230	3.60	4.01	10.148
25	62	4.55	0.083	0.157	0.121	0.84	0.32	0.47	0.55	1.36	1.82	2.7	83000	0.229	2.99	2.66	3.231
25	62	4.55	0.079	0.144	0.113	0.75	0.28	0.40	0.55	1.36	1.74	2.6	79000	0.215	2.78	2.48	2.901
25	62	4.55	0.077	0.139	0.108	0.78	0.27	0.38	0.55	1.36	1.69	2.5	77000	0.223	2.73	2.37	2.792
25	62	4.17	0.081	0.164	0.127	0.92	0.34	0.43	0.60	1.49	1.94	3.0	81000	0.226	2.62	3.05	4.114
25	62	4.17	0.077	0.154	0.119	0.81	0.32	0.45	0.60	1.49	1.85	2.9	77000	0.227	2.92	2.85	3.685
25	62	4.17	0.075	0.149	0.111	0.84	0.33	0.48	0.60	1.49	1.80	2.8	75000	0.255	3.22	2.66	3.788
25	62	3.85	0.079	0.168	0.128	0.80	0.34	0.45	0.65	1.61	2.05	3.3	79000	0.238	2.68	3.32	5.537
25	62	3.85	0.075	0.150	0.116	0.88	0.31	0.44	0.65	1.61	1.95	3.2	75000	0.227	2.93	3.01	5.348
25	62	3.85	0.072	0.145	0.114	0.77	0.30	0.42	0.65	1.61	1.87	3.0	72000	0.214	2.90	2.96	4.498
25	62	3.57	0.077	0.171	0.133	0.95	0.35	0.51	0.70	1.74	2.16	3.6	77000	0.222	2.98	3.73	6.556
25	62	3.57	0.075	0.159	0.126	0.91	0.32	0.49	0.70	1.74	2.10	3.5	75000	0.208	3.08	3.53	6.607
25	62	3.57	0.072	0.152	0.115	0.87	0.31	0.40	0.70	1.74	2.02	3.4	72000	0.243	2.63	3.22	6.641
25	62	3.33	0.075	0.174	0.137	0.94	0.34	0.54	0.75	1.86	2.25	3.9	75000	0.213	3.10	4.11	7.582
25	62	3.33	0.072	0.158	0.122	0.83	0.35	0.46	0.75	1.86	2.16	3.8	72000	0.228	2.91	3.66	8.387
25	62	3.33	0.069	0.151	0.119	0.90	0.33	0.42	0.75	1.86	2.07	3.6	69000	0.212	2.78	3.57	7.160
25	75	4.55	0.083	0.157	0.124	0.84	0.31	0.44	0.55	1.65	1.82	2.7	83000	0.210	2.80	2.73	3.012
25	75	4.55	0.079	0.144	0.111	0.75	0.28	0.39	0.55	1.65	1.74	2.6	79000	0.229	2.71	2.44	3.019
25	75	4.55	0.077	0.139	0.107	0.78	0.29	0.38	0.55	1.65	1.69	2.5	77000	0.230	2.73	2.35	2.845
25	75	4.17	0.081	0.164	0.127	0.92	0.33	0.42	0.60	1.80	1.94	3.0	81000	0.226	2.56	3.05	4.114
25	75	4.17	0.077	0.154	0.121	0.81	0.31	0.40	0.60	1.80	1.85	2.9	77000	0.214	2.60	2.90	3.505

t	s	y_1	q	y_{2^*}	y_2	L_{j^*}	L_{rj}	L_j	t/y_1	s/y_1	U_1	F_1	R_1	$(y_{2^*}-y_2)/y_{2^*}$	L_j/y_{2^*}	y_2/y_1	ε
(mm)	(mm)	(cm)	($m^3/s/m$)	(m)	(m)	(m)	(m)	(m)			(m/s)						
25	125	3.57	0.077	0.171	0.125	0.95	0.34	0.52	0.70	3.50	2.16	3.6	77000	0.269	3.04	3.50	7.719
25	125	3.57	0.075	0.159	0.121	0.91	0.35	0.46	0.70	3.50	2.10	3.5	75000	0.239	2.89	3.39	7.280
25	125	3.57	0.072	0.152	0.114	0.87	0.32	0.42	0.70	3.50	2.02	3.4	72000	0.250	2.76	3.19	6.757
25	125	3.33	0.075	0.174	0.124	0.94	0.40	0.52	0.75	3.75	2.25	3.9	75000	0.287	2.99	3.72	9.850
25	125	3.33	0.072	0.158	0.119	0.83	0.35	0.47	0.75	3.75	2.16	3.8	72000	0.247	2.97	3.57	8.842
25	125	3.33	0.069	0.151	0.115	0.90	0.33	0.40	0.75	3.75	2.07	3.6	69000	0.238	2.65	3.45	7.748
35	140	6.36	0.093	0.147	0.109	0.57	0.30	0.39	0.55	2.20	1.46	1.9	93000	0.259	2.65	1.71	0.918
35	140	6.36	0.091	0.140	0.107	0.52	0.28	0.37	0.55	2.20	1.43	1.8	91000	0.236	2.64	1.68	0.831
35	140	6.36	0.087	0.134	0.103	0.50	0.27	0.36	0.55	2.20	1.37	1.7	87000	0.231	2.69	1.62	0.672
35	140	5.83	0.089	0.144	0.107	0.55	0.32	0.42	0.60	2.40	1.53	2.0	89000	0.257	2.92	1.84	1.341
35	140	5.83	0.085	0.134	0.105	0.54	0.31	0.40	0.60	2.40	1.46	1.9	85000	0.216	2.99	1.80	1.062
35	140	5.83	0.081	0.128	0.097	0.48	0.28	0.38	0.60	2.40	1.39	1.8	81000	0.242	2.97	1.66	0.925
35	140	5.38	0.087	0.148	0.108	0.68	0.32	0.43	0.65	2.60	1.62	2.2	87000	0.270	2.91	2.01	1.943
35	140	5.38	0.083	0.137	0.103	0.60	0.32	0.41	0.65	2.60	1.54	2.1	83000	0.248	2.99	1.91	1.643
35	140	5.38	0.079	0.122	0.098	0.52	0.31	0.42	0.65	2.60	1.47	2.0	79000	0.197	3.44	1.82	1.367
35	140	5.00	0.085	0.155	0.113	0.67	0.35	0.46	0.70	2.80	1.70	2.4	85000	0.271	2.97	2.26	2.462
35	140	5.00	0.081	0.145	0.109	0.63	0.34	0.45	0.70	2.80	1.62	2.3	81000	0.248	3.10	2.18	2.040
35	140	5.00	0.077	0.136	0.105	0.56	0.29	0.42	0.70	2.80	1.54	2.2	77000	0.228	3.09	2.10	1.655
35	140	4.67	0.083	0.158	0.113	0.71	0.36	0.48	0.75	3.00	1.78	2.6	83000	0.285	3.04	2.42	3.236
35	140	4.67	0.079	0.140	0.108	0.66	0.31	0.43	0.75	3.00	1.69	2.5	79000	0.229	3.07	2.31	2.743
35	140	4.67	0.077	0.135	0.104	0.69	0.31	0.44	0.75	3.00	1.65	2.4	77000	0.230	3.26	2.23	2.580

APPENDIX - II

t	s	y_1	q	y_{2^*}	y_2	L_{rj}	L_j	t/y_1	s/y_1	U_1	F_1	R_1	$(y_{2^*}-y_2)/y_{2^*}$	L_j/y_{2^*}	ε
(mm)	(mm)	(cm)	($m^3/s/m$)	(m)	(m)	(m)	(m)			(m/s)					
13	68	2.54	0.051	0.132	0.104	0.31	0.41	0.50	2.68	2.00	4	50800	0.209	3.10	8.420
13	68	2.54	0.063	0.167	0.128	0.41	0.48	0.50	2.68	2.50	5	63500	0.235	2.84	15.683
13	68	2.54	0.076	0.203	0.145	0.48	0.54	0.50	2.68	3.00	6	76200	0.286	2.68	27.799
13	68	2.54	0.089	0.239	0.188	0.61	0.75	0.50	2.68	3.49	7	88646	0.216	3.13	31.232
13	68	2.54	0.101	0.275	0.200	0.65	0.85	0.50	2.68	3.99	8	101346	0.273	3.09	50.744
13	68	2.54	0.114	0.311	0.233	0.88	1.02	0.50	2.68	4.49	9	114046	0.252	3.28	61.515
13	68	2.54	0.127	0.347	0.263	1.02	1.09	0.50	2.68	4.99	10	126746	0.243	3.14	74.843
13	68	50.8	0.143	0.263	0.210	0.75	0.88	0.25	1.34	2.82	4	143256	0.202	3.36	8.170
13	68	50.8	0.207	0.390	0.310	1.22	1.29	0.25	1.34	4.07	5.8	206756	0.205	3.31	19.435
22	68	50.8	0.143	0.263	0.210	0.61	0.82	0.43	1.34	2.82	4	143256	0.202	3.10	8.170
22	68	50.8	0.207	0.390	0.310	1.02	1.29	0.43	1.34	4.07	5.8	206756	0.205	3.31	19.435

APPENDIX - III

t	s	y_1	q	y_{2*}	y_2	L_{j*}	L_{rj}	L_j	t/y_1	s/y_1	U_1	F_1	R_1	$(y_{2*}-y_2)/y_{2*}$	L_j/y_{2*}	y_2/y_1	ε
(mm)	(mm)	(cm)	($m^3/s/m$)	(m)	(m)	(m)	(m)	(m)			(m/s)						
15	75	2.17	0.042	0.125	0.116	0.675	0.34	0.44	0.70	3.46	2.00	4.4	43400	0.072	3.52	5.35	1.035
15	75	3.49	0.069	0.151	0.122	0.731	0.37	0.46	0.43	3.61	1.99	3.4	69451	0.192	3.05	3.50	5.082
15	75	7.50	0.164	0.198	0.186	1.08	0.45	0.58	0.20	1	2.19	2.6	164250	0.061	2.93	2.48	2.606